

On the Coexistence Between Full-Duplex and NOMA

Zhiguo Ding¹, Senior Member, IEEE, Pingzhi Fan, Fellow, IEEE, and H. Vincent Poor², Fellow, IEEE

Abstract—The purpose of this letter is to investigate the feasibility of full-duplex non-orthogonal multiple access (FD-NOMA), where uplink and downlink NOMA transmissions are carried out at the same time. Analytical and simulation results are provided to demonstrate that FD-NOMA can offer significant performance gains over half-duplex NOMA and orthogonal multiple access, provided that co-channel interference is sufficiently suppressed.

Index Terms—Non-orthogonal multiple access, full-duplex, joint uplink and downlink transmission.

I. INTRODUCTION

BOTH non-orthogonal multiple access (NOMA) and full-duplex (FD) have been recognized as important enabling techniques for future wireless communication systems [1]–[3]. Naturally it is important to investigate the coexistence of these two important communication techniques. Interestingly, most existing works have mainly focused on the application of FD to cooperative NOMA [4]–[6]. In addition to cooperative NOMA, FD can also be used to realize simultaneous NOMA uplink and downlink transmissions. This type of FD-NOMA effectively ensures spectrum sharing among the uplink and downlink users and avoids the situation in which downlink (or uplink) users with poor channel conditions solely occupy the scarce bandwidth. In [7], power allocation as well as subcarrier allocation have been investigated in this FD-NOMA scenario, and its multi-cell extension has been considered in [8].

However, there is still a lack of theoretic studies to rigorously demonstrate the feasibility of FD-NOMA, which is the motivation of this letter. Particularly, we consider a communication system with a FD base station (BS) and multiple HD users, where NOMA uplink and downlink transmissions can be carried out simultaneously. This FD-NOMA scheme is particularly important to the scenario in which downlink (or uplink) users have poor channel conditions, where the use of FD techniques avoids the spectrum to be solely occupied by these users. However, FD-NOMA can potentially cause strong co-channel interference at both uplink and downlink

transmissions. For example, for the uplink transmission, the residual self-interference caused by FD can degrade the reception reliability of the BS, whereas for the downlink transmission, signals from uplink users cause strong interference to the downlink users. Analytical and simulation results are provided to illustrate the impact of these interference on uplink and downlink transmissions, and demonstrate that FD-NOMA can offer significant performance gains over HD-NOMA and orthogonal multiple access (OMA), provided that the co-channel interference is sufficiently suppressed.

II. SYSTEM MODEL

Consider a communication network with one FD BS, M uplink users and one downlink user. As shown in Fig. 1, assume that the downlink user is located at $(-d_0, 0)$, and the M uplink users are uniformly deployed in a sectorized annulus, with outer radius r_1 , inner radius r_2 and angle $[-\frac{1}{2}\theta, \frac{1}{2}\theta]$, where $\theta \leq \pi$. The reason for focusing on this scenario is explained in the following. In particular, the downlink user can be viewed as a typical cell-edge user, i.e., its connection to the BS is poor. For this scenario, the use of HD-NOMA or OMA results in a situation in which a dedicated bandwidth resource, such as a time slot, is allocated to this downlink cell-edge user. As a result, the spectral efficiency is low since this scarce bandwidth resource is solely occupied by this user. The use of FD can avoid this spectral inefficiency, where the spectrum that is solely occupied by the downlink user in the HD mode can be released to the uplink users. The reason for the considered uplink user deployment is to ensure that the uplink users are not too close to the downlink user.

When the FD-NOMA principle is used, all the downlink and uplink users are served simultaneously. Therefore, at the end of the joint uplink-downlink transmission, the BS receives $y_{BS} = \sum_{m=1}^M \sqrt{P_U} h_m s_m + h_{SI} \sqrt{P_{SI}} s_0 + n_{BS}$, and the downlink user receives $y_D = h_0 \sqrt{P_{BS}} s_0 + \sqrt{P_U} \sum_{i=1}^M g_m s_m + n_D$, where s_0 denotes the downlink signal, s_m denotes the uplink message, h_m denotes the channel gain between the BS and uplink user m , h_{SI} denotes the self-interference channel gain, g_m denotes the channel gain between uplink user m and the downlink user, n_D and n_{BS} denote the noise for downlink and uplink transmissions, respectively. Note that we assume that self-interference cannot be completely cancelled due to imperfect hardware impairments [4]–[9]. P_U and P_{BS} denote the transmission power of the users and the BS, respectively. P_{SI} denotes the power of the residual self interference. If the area of the annulus is small, it is reasonable to assume that all the users have the same transmission power. Note that the transmission powers of the users are not necessarily the same, particularly if the area of the annulus is large, and the use of optimal power allocation can further improve the performance of the proposed FD-NOMA scheme, which is an important direction of future research. It is assumed that h_{SI} is complex Gaussian distributed with zero mean and unit variance, and a composite model is used for h_m , i.e., each user experiences path loss as well as identically distributed multi-path fading.

Manuscript received November 30, 2017; revised February 3, 2018; accepted February 19, 2018. Date of publication March 2, 2018; date of current version October 11, 2018. The work of Z. Ding was supported by the U.K. EPSRC under Grant EP/L025272/1 and Grant EP/N005597/1. The work of P. Fan was supported in part by NSFC Key Project under Grant 61731017, and in part by the 111 Project under Grant 111-2-14. The work of H. V. Poor was supported by the U.S. National Science Foundation under Grant CNS-1702808 and Grant ECCS-1647198. The associate editor coordinating the review of this paper and approving it for publication was T. Riihonen. (Corresponding author: Zhiguo Ding.)

Z. Ding is with the Department of Electrical Engineering, Princeton University, Princeton, NJ 08544 USA, and also with SCC, Lancaster University, Lancaster LA14WA, U.K. (e-mail: z.ding@lancaster.ac.uk).

P. Fan is with the Institute of Mobile Communications, Southwest Jiaotong University, Chengdu 611756, China.

H. V. Poor is with the Department of Electrical Engineering, Princeton University, Princeton, NJ 08544 USA.

Digital Object Identifier 10.1109/LWC.2018.2811492

2162-2345 © 2018 IEEE. Personal use is permitted, but republication/redistribution requires IEEE permission.

See http://www.ieee.org/publications_standards/publications/rights/index.html for more information.

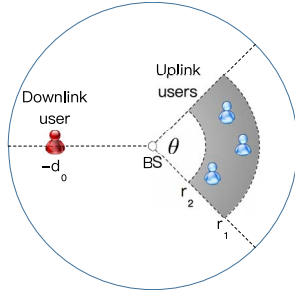


Fig. 1. An illustration for the considered FD-NOMA scenario. The downlink user is located at $(-d_0, 0)$ and the uplink users are uniformly deployed in a sectored annulus, with outer radius r_1 , inner radius r_2 and angle θ .

III. PERFORMANCE ANALYSIS

A. Performance of Uplink Transmission

The uplink sum rate achieved by successive interference cancellation (SIC) can be expressed as follows [10]:

$$R_{\text{FD}}^{\text{U}} = \log \left(1 + \frac{\sum_{m=1}^M P_{\text{U}} |h_m|^2}{P_{\text{SI}} |h_{\text{SI}}|^2 + 1} \right), \quad (1)$$

where we assume that the noise power is normalized. On the other hand, the sum rate of HD-NOMA is given by

$$R_{\text{HD}}^{\text{U}} = \frac{1}{2} \log \left(1 + \sum_{m=1}^M P_{\text{U}} |h_m|^2 \right) \quad (2)$$

where the term $\frac{1}{2}$ is due to the fact that the uplink transmission can use only half of the bandwidth. The sum rate of OMA will be $R_{\text{OMA}}^{\text{U}} = \frac{1}{2M} \sum_{m=1}^M \log(1 + P_{\text{U}} |h_m|^2)$. From the capacity region of multiple access channels, we learn that $R_{\text{HD}}^{\text{U}} \geq R_{\text{OMA}}^{\text{U}}$. Therefore, in this letter, we mainly focus on the comparison between R_{FD}^{U} and R_{HD}^{U} , i.e., the following probability $P^{\text{U}} \triangleq \text{P}(R_{\text{FD}}^{\text{U}} \leq R_{\text{HD}}^{\text{U}})$, which is studied in the following theorem.

Theorem 1: The probability that FD-NOMA yields worse performance than HD-NOMA can be approximated as follows:

$$\begin{aligned} P^{\text{U}} &\approx \sum_{k_1 + \dots + k_n = M} \binom{M}{k_1, \dots, k_n} \\ &\times \sum_{n=1, k_n \neq 0}^N \sum_{i_n=0}^{k_n-1} \frac{2P_{\text{SI}}^2 A_{i_n}}{P_{\text{U}}(k_n - i_n - 1)!} \\ &\times \frac{e^{-\frac{1}{P_{\text{SI}}}}}{P_{\text{U}}^{k_n - i_n - 1} P_{\text{SI}}^2} \sum_{p=0}^{k_n - i_n - 1} \binom{k_n - i_n - 1}{p} 2^{k_n - i_n - 1 - p} \\ &\times [\phi(p + k_n - i_n + 1) - \phi(p + k_n - i_n)], \end{aligned} \quad (3)$$

where N is the Chebyshev-Gauss approximation parameter, $b_n = \frac{\pi}{N(r_1 + r_2)} \left(\frac{r_1 + r_2}{2} + \frac{r_1 - r_2}{2} \theta_n \right) \sqrt{1 - \theta_n^2}$, $c_n = \left(\frac{r_1 + r_2}{2} + \frac{r_1 - r_2}{2} \theta_n \right)^\alpha$, $\theta_n = \cos\left(\frac{2n-1}{2N}\pi\right)$, $A_{i_n} = \frac{1}{i_n!} \frac{d^{i_n}}{ds^{i_n}} [(s + c_n)^{k_n} q(s)]|_{s=-c_n}$, $q(s) = \prod_{n=1, k_n \neq 0}^N \frac{b_n^{k_n} c_n^{k_n}}{(c_n + s)^{k_n}}$,

$$\begin{aligned} \phi(l) &= (l-1)! \left(\frac{2c_n}{P_{\text{U}}} \right)^{-\frac{1}{2}} e^{\frac{\left(\frac{2c_n}{P_{\text{U}}} + \frac{1}{P_{\text{SI}}} \right)^2}{8} \frac{P_{\text{U}}}{c_n}} \\ &\times D_{-l} \left(\frac{\left(\frac{2c_n}{P_{\text{U}}} + \frac{1}{P_{\text{SI}}} \right) \sqrt{P_{\text{U}}}}{\sqrt{2}} \frac{1}{\sqrt{c_n}} \right) \end{aligned} \quad (4)$$

and $D_{-l}(\cdot)$ denotes a parabolic cylinder functions.

Proof: Define $x = \sum_{m=1}^M |h_m|^2$ and $y = |h_0|^2$. The theorem is proved by first showing the outage probability as a function of x and y and then characterizing the density functions of the two variables, where the key steps are to find the density function of $|h_m|^2$ and apply the Laplace transform to characterize the density function of x . The probability P^{U} can be expressed as follows:

$$P^{\text{U}} = \text{P} \left(\log \left(1 + \frac{P_{\text{U}} x}{P_{\text{SI}} y + 1} \right) \leq \frac{1}{2} \log(1 + P_{\text{U}} x) \right). \quad (5)$$

With some algebraic manipulations, P^{U} can be rewritten as follows:

$$P^{\text{U}} = \text{P} \left(x \leq \frac{P_{\text{SI}}^2 y^2 - 1}{P_{\text{U}}} \right). \quad (6)$$

If $y < \frac{1}{P_{\text{SI}}}$, $R_{\text{FD}}^{\text{U}} \geq R_{\text{HD}}^{\text{U}}$ always holds, i.e., FD-NOMA can always yield a larger sum rate than HD-NOMA. Therefore the probability can be expressed as follows:

$$\begin{aligned} P^{\text{U}} &= \mathcal{E}_{y > \frac{1}{P_{\text{SI}}}} \left\{ F_x \left(\frac{P_{\text{SI}}^2 y^2 - 1}{P_{\text{U}}} \right) \right\} \\ &= \int_{\frac{1}{P_{\text{SI}}}}^{\infty} F_x \left(\frac{P_{\text{SI}}^2 y^2 - 1}{P_{\text{U}}} \right) e^{-y} dy, \end{aligned} \quad (7)$$

where $F_x(x)$ and $f_x(x)$ denote the cumulative distribution function (CDF) and probability density function (PDF) of x .

Although each user is uniformly deployed in the sectored annulus shown in Fig. 1, denoted by \mathcal{A} , instead of a disc, the steps to find the PDF of a composite channel gain in [2] are still applicable. In particular, recall that a composite channel model is assumed, i.e., $h_m = \frac{\bar{h}_m}{d_m^\alpha}$, where \bar{h}_m denotes identically distributed Rayleigh fading, d_m denotes the distance between uplink user m to the BS, and α denotes the path loss exponent. By using the characteristics of Rayleigh fading, the CDF of the composite channel gain can be expressed as follows:

$$F_{|h_m|^2}(y) = \int_{\mathcal{A}} \left(1 - e^{-d_m^\alpha y} \right) p_W(w) dw, \quad (8)$$

where W denotes the location of a user and $p_W(w)$ denotes the PDF of W . Note that d_m is decided by the location of uplink user m . Since each uplink user is uniformly distributed in \mathcal{A} , the PDF of the location of a user is given by $p_W(w) = \frac{2}{\theta(r_1^2 - r_2^2)}$.

Therefore, the CDF can be expressed as follows:

$$\begin{aligned} F_{|h_m|^2}(y) &= \int_{-\frac{\theta}{2}}^{\frac{\theta}{2}} \int_{r_2}^{r_1} \frac{2(1 - e^{-r^\alpha y})}{\theta(r_1^2 - r_2^2)} r dr d\theta \\ &= 1 - \frac{2}{(r_1^2 - r_2^2)} \int_{r_2}^{r_1} e^{-r^\alpha y} r dr. \end{aligned} \quad (9)$$

The Chebyshev-Gauss approximation can be applied to obtain the following:

$$\begin{aligned} F_{|h_m|^2}(y) &= 1 - \frac{2}{(r_1^2 - r_2^2)} \int_{-1}^1 e^{-\left(\frac{r_1 + r_2}{2} + \frac{r_1 - r_2}{2} x \right)^\alpha y} \\ &\times \left(\frac{r_1 + r_2}{2} + \frac{r_1 - r_2}{2} x \right) \frac{r_1 - r_2}{2} dx \approx 1 - \sum_{n=1}^N b_n e^{-c_n y}. \end{aligned}$$

Therefore, the PDF of the channel gains is $f_{|h_m|^2}(y) \approx \sum_{n=1}^N b_n c_n e^{-c_n y}$. Note that these approximated expressions are

sums of exponential functions, which are preferable forms for the following Laplace analysis. Particularly, the Laplace transform for the PDF of $|h_m|^2$ is given by

$$\mathcal{L}(f_{|h_m|^2}(y)) \approx \sum_{n=1}^N \frac{b_n c_n}{c_n + s}. \quad (10)$$

Since all the uplink users' channels are independent and identically distributed, the PDF of the sum of the channel gains, $\sum_{m=1}^M |h_m|^2$, has the following Laplace transform:

$$\begin{aligned} \mathcal{L}(f_x(x)) &\approx \left(\sum_{n=1}^N \frac{b_n c_n}{c_n + s} \right)^M \\ &= \sum_{k_1 + \dots + k_n = M} \binom{M}{k_1, \dots, k_n} \prod_{n=1}^N \frac{b_n^{k_n} c_n^{k_n}}{(c_n + s)^{k_n}}. \end{aligned} \quad (11)$$

Note that some k_n might be zero, which means that the corresponding term $\frac{b_n^{k_n} c_n^{k_n}}{(c_n + s)^{k_n}}$ becomes one, i.e., this term has no impact on the inverse Laplace transform. Therefore, $\mathcal{L}(f_x(x))$ can be further rewritten as follows:

$$\mathcal{L}(f_x(x)) \approx \sum_{k_1 + \dots + k_n = M} \binom{M}{k_1, \dots, k_n} \prod_{n=1, k_n \neq 0}^N \frac{b_n^{k_n} c_n^{k_n}}{(c_n + s)^{k_n}}.$$

By applying the partial fraction, the Laplace transform can be rewritten as follows:

$$\begin{aligned} \mathcal{L}(f_x(x)) &\approx \sum_{k_1 + \dots + k_n = M} \binom{M}{k_1, \dots, k_n} \\ &\times \sum_{n=1, k_n \neq 0}^N \sum_{i_n=0}^{k_n-1} \frac{A_{i_n}}{(c_n + s)^{k_n - i_n}}. \end{aligned} \quad (12)$$

After applying the inverse Laplace transform, the PDF of the sum of the channel gains can be obtained as follows:

$$\begin{aligned} f_x(x) &\approx \sum_{k_1 + \dots + k_n = M} \binom{M}{k_1, \dots, k_n} \\ &\times \sum_{n=1, k_n \neq 0}^N \sum_{i_n=0}^{k_n-1} \frac{A_{i_n} x^{k_n - i_n - 1} e^{-c_n x}}{(k_n - i_n - 1)!}. \end{aligned} \quad (13)$$

In order to use the PDF of $\sum_{m=1}^M |h_m|^2$ directly, we rewrite the probability P^U as follows:

$$\begin{aligned} P^U &= \int_{\frac{1}{P_{SI}}}^{\infty} F_x \left(\frac{P_{SI}^2 y^2 - 1}{P_U} \right) e^{-y} dy \\ &= \frac{2P_{SI}^2}{P_U} \int_{\frac{1}{P_{SI}}}^{\infty} f_x \left(\frac{P_{SI}^2 y^2 - 1}{P_U} \right) e^{-y} y dy. \end{aligned} \quad (14)$$

By substituting the PDF of $\sum_{m=1}^M |h_m|^2$, we can have

$$\begin{aligned} P^U &\approx \sum_{k_1 + \dots + k_n = M} \binom{M}{k_1, \dots, k_n} \\ &\times \sum_{n=1, k_n \neq 0}^N \sum_{i_n=0}^{k_n-1} \frac{2P_{SI}^2 A_{i_n}}{P_U (k_n - i_n - 1)!} \\ &\times \underbrace{\int_{\frac{1}{P_{SI}}}^{\infty} \left(\frac{P_{SI}^2 y^2 - 1}{P_U} \right)^{k_n - i_n - 1} e^{-c_n \left(\frac{P_{SI}^2 y^2 - 1}{P_U} \right)} y e^{-y} dy}_{Q_1}. \end{aligned} \quad (15)$$

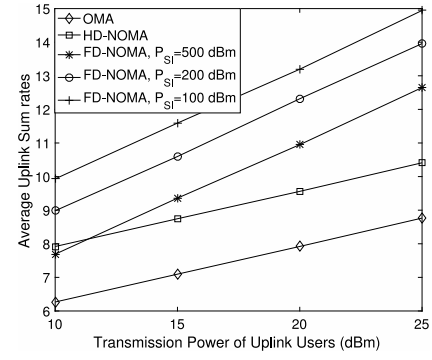


Fig. 2. The uplink sum rates achieved by the three transmission schemes. $\alpha = 4$, $r_1 = 10$, $r_2 = 0$ and $\theta = \frac{\pi}{8}$.

Define $t = P_{SI}y - 1$, and the term Q_1 can be rewritten as follows:

$$\begin{aligned} Q_1 &= \int_0^{\infty} \left(\frac{t^2 + 2t}{P_U} \right)^{k_n - i_n - 1} e^{-c_n \left(\frac{t^2 + 2t}{P_U} \right)} \frac{t + 1}{P_{SI}^2} e^{-\frac{t+1}{P_{SI}}} dt \\ &= \frac{e^{-\frac{1}{P_{SI}}}}{P_U^{k_n - i_n - 1} P_{SI}^2} \int_0^{\infty} t^{k_n - i_n - 1} e^{-\frac{c_n}{P_U} (t^2 + 2t) - \frac{t}{P_{SI}}} dt \\ &\quad \times (t + 2)^{k_n - i_n - 1} (t + 1) dt \\ &= \frac{e^{-\frac{1}{P_{SI}}}}{P_U^{k_n - i_n - 1} P_{SI}^2} \sum_{p=0}^{k_n - i_n - 1} \binom{k_n - i_n - 1}{p} 2^{k_n - i_n - 1 - p} \\ &\quad \times \int_0^{\infty} t^{p + k_n - i_n - 1} (t + 1) e^{-\frac{c_n}{P_U} t^2 - \left(\frac{2c_n}{P_U} + \frac{1}{P_{SI}} \right) t} dt \end{aligned} \quad (16)$$

After applying [11, eq. (3.462.1)], the term Q_1 can be obtained as follows:

$$\begin{aligned} Q_1 &= \frac{e^{-\frac{1}{P_{SI}}}}{P_U^{k_n - i_n - 1} P_{SI}^2} \sum_{p=0}^{k_n - i_n - 1} \binom{k_n - i_n - 1}{p} 2^{k_n - i_n - 1 - p} \\ &\quad \times [\phi(p + k_n - i_n + 1) - \phi(p + k_n - i_n)], \end{aligned}$$

where $\phi(\cdot)$ is defined in the theorem. By combining (15) with (16), the theorem is proved. ■

B. The Performance of Downlink Transmission

The rate of the downlink user can be expressed as follows:

$$R_{FD}^D = \log \left(1 + \frac{P_{BS} |h_0|^2}{P_U \sum_{i=1}^M |g_m|^2 + 1} \right). \quad (17)$$

Similar to P_U , the following probability is of interest:

$$P_D \triangleq P(R_{FD}^D < R_{HD}^D), \quad (18)$$

where $R_{HD}^D = \frac{1}{2} \log(1 + P_{BS} |h_0|^2)$. Following steps similar to those in the previous subsection, this probability can be rewritten as follows:

$$\begin{aligned} P^D &= P \left(|h_0|^2 \leq \frac{P_U^2 z^2 - 1}{P_{BS}} \right) \\ &= 1 - F_z \left(\frac{1}{P_U} \right) - \int_{\frac{1}{P_U}}^{\infty} e^{-\frac{d_0^\alpha (P_U^2 z^2 - 1)}{P_{BS}}} f_z(z) dz, \end{aligned} \quad (19)$$

where $z = \sum_{i=1}^M |g_m|^2$, $F_z(z)$ and $f_z(z)$ denote the CDF and PDF of z , respectively. Compared to $\sum_{i=1}^M |h_m|^2$, the PDF

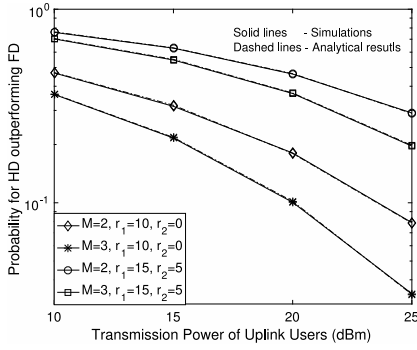


Fig. 3. The probability $P(R_{FD}^U \leq R_{HD}^U)$ versus the user transmission power. $N = 20$, $\alpha = 4$, $\theta = \frac{\pi}{8}$ and $P_{SI} = 200$ dBm.

of $\sum_{i=1}^M |g_m|^2$ is more challenging to obtain, mainly due to the characteristics of the distances between the uplink users and the downlink user. Because of the network topology considered in Fig. 1, the distances from the uplink users to the downlink user are smaller than or at least equal to d_0 , since $\theta \leq \pi$. Therefore, by keeping the small scale Rayleigh fading part of g_m the same and replacing its path loss with d_0^α , the following upper bound on the probability can be obtained:

$$P^D \leq 1 - \frac{\gamma\left(M, \frac{d_0^\alpha}{P_U}\right)}{(M-1)!} - \int_{\frac{1}{P_U}}^{\infty} e^{-\frac{d_0^\alpha (P_U^2 z^2 - 1)}{P_{BS}}} \tilde{f}_z(z) dz, \quad (20)$$

where $\tilde{f}_z(z) = \frac{d_0^{\alpha M}}{(M-1)!} z^{M-1} e^{-d_0^\alpha z}$. With some manipulations, the upper bound can be obtained as follows:

$$\begin{aligned} P^D \geq 1 - \frac{\gamma\left(M, \frac{d_0^\alpha}{P_U}\right)}{(M-1)!} - \frac{d_0^{\alpha M} e^{-\frac{d_0^\alpha}{P_U}}}{(M-1)! P_U^M} \sum_{p=0}^{M-1} \binom{M-1}{p} \\ \times p! \left(\frac{2d_0^\alpha}{P_{BS}}\right)^{-\frac{p+1}{2}} e^{\frac{P_{BS}}{8d_0^\alpha} \left(\frac{2d_0^\alpha}{P_{BS}} + \frac{d_0^\alpha}{P_U}\right)^2} \\ \times D_{-(p+1)}\left(\frac{\sqrt{P_{BS}}}{\sqrt{2d_0^\alpha}} \left(\frac{2d_0^\alpha}{P_{BS}} + \frac{d_0^\alpha}{P_U}\right)\right). \end{aligned} \quad (21)$$

IV. NUMERICAL RESULTS

In Fig. 2, the average uplink sum rates achieved by FD-NOMA, HD-NOMA and OMA are compared. As can be observed from the figure, the use of FD can yield a significant improvement in terms of the uplink sum rate, compared to HD-NOMA and OMA. Another important observation from Fig. 2 is that the power of the residual self interference has a crucial impact on the performance of FD-NOMA. Fig. 3 illustrates that the number of uplink users and the locations of these users also have significant impacts on the performance gain of FD-NOMA over HD-NOMA. Particularly, increasing the number of uplink users (or having uplink users closer to the BS) is helpful to reduce the probability, $P(R_{FD}^U \leq R_{HD}^U)$, since $P(R_{FD}^U \leq R_{HD}^U) = P(\sum_{m=1}^M |h_m|^2 \leq \frac{P_{SI}^2 |h_0|^4 - 1}{P_U})$ and increasing M (or reducing the distances between the BS and the users) can increase the value of $\sum_{m=1}^M |h_m|^2$. Fig. 3 also shows that the analytical results developed in Theorem 1 match perfectly the simulation results, with a choice of $N = 20$.

Fig. 4 demonstrates the impact of FD-NOMA on the downlink rate. In particular, Fig. 4 shows that having more uplink users to participate in FD-NOMA decreases the downlink rate, since the uplink transmissions cause more interference to the

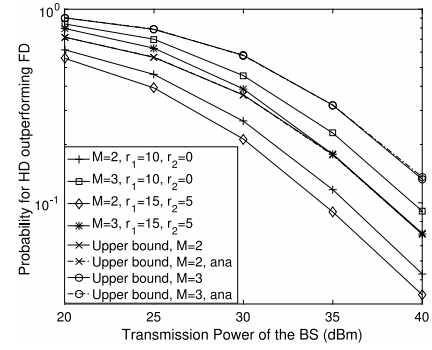


Fig. 4. The probability $P(R_{FD}^D \leq R_{HD}^D)$ versus the user transmission power. $N = 20$, $\alpha = 4$, $\theta = \frac{\pi}{8}$ and $P_U = 20$ dBm.

downlink user. Fig. 4 also illustrates the impacts of r_0 and r_1 on the downlink performance. Particularly, reducing r_0 and r_1 , i.e., having the uplink users closer to the BS, deteriorates the downlink outage probability, since reducing r_0 and r_1 makes the uplink interference to the downlink user stronger. The analytical results for the proposed upper bound on P^D are shown to match the simulation results in the figure, and the upper bound becomes tighter if the number of uplink users increases and these users move towards the BS.

V. CONCLUSION

This letter studied the performance of FD-NOMA, where uplink and downlink NOMA transmissions are carried out at the same time. Analytical and simulation results have been developed to demonstrate that FD-NOMA can offer significant performance gains over HD-NOMA and OMA, provided that co-channel interference is sufficiently suppressed.

REFERENCES

- [1] Y. Saito, A. Benjebbour, Y. Kishiyama, and T. Nakamura, "System-level performance evaluation of downlink non-orthogonal multiple access (NOMA)," in *Proc. IEEE Int. Symp. Pers. Indoor Mobile Radio Commun.*, London, U.K., Sep. 2013, pp. 611–615.
- [2] Z. Ding, Z. Yang, P. Fan, and H. V. Poor, "On the performance of non-orthogonal multiple access in 5G systems with randomly deployed users," *IEEE Signal Process. Lett.*, vol. 21, no. 12, pp. 1501–1505, Dec. 2014.
- [3] J. Lee and T. Q. S. Quek, "Hybrid full/half-duplex system analysis in heterogeneous wireless networks," *IEEE Trans. Wireless Commun.*, vol. 14, no. 5, pp. 2883–2895, May 2015.
- [4] Z. Zhang, Z. Ma, M. Xiao, Z. Ding, and P. Fan, "Full-duplex device-to-device-aided cooperative non-orthogonal multiple access," *IEEE Trans. Veh. Technol.*, vol. 66, no. 5, pp. 4467–4471, May 2017.
- [5] L. Zhang *et al.*, "Performance analysis and optimization in downlink NOMA systems with cooperative full-duplex relaying," *IEEE J. Sel. Areas Commun.*, vol. 35, no. 10, pp. 2398–2412, Oct. 2017.
- [6] C. Zhong and Z. Zhang, "Non-orthogonal multiple access with cooperative full-duplex relaying," *IEEE Commun. Lett.*, vol. 20, no. 12, pp. 2478–2481, Dec. 2016.
- [7] Y. Sun, D. W. K. Ng, Z. Ding, and R. Schober, "Optimal joint power and subcarrier allocation for full-duplex multicarrier non-orthogonal multiple access systems," *IEEE Trans. Commun.*, vol. 65, no. 3, pp. 1077–1091, Mar. 2017.
- [8] M. S. Elbamy, M. Bennis, W. Saad, M. Debbah, and M. Latva-Aho, "Resource optimization and power allocation in in-band full duplex-enabled non-orthogonal multiple access networks," *IEEE J. Sel. Areas Commun.*, vol. 35, no. 12, pp. 2860–2873, Dec. 2017.
- [9] K. Alexandris, A. Balatsoukas-Stimming, and A. Burg, "Measurement-based characterization of residual self-interference on a full-duplex MIMO testbed," in *Proc. IEEE Sensor Array Multichannel Signal Process. Workshop (SAM)*, A Coruña, Spain, Jun. 2014, pp. 329–332.
- [10] T. Cover and J. Thomas, *Elements of Information Theory*, 6th ed. New York, NY, USA: Wiley, 1991.
- [11] I. S. Gradshteyn and I. M. Ryzhik, *Table of Integrals, Series and Products*, 6th ed. New York, NY, USA: Academic Press, 2000.